



HAL
open science

Pcl covered pp meshes plasma-grafted by sulfonated monomer for the prevention of postoperative abdominal adhesions

Malo Dufay, Maude Jimenez, Mathilde Casetta, Feng Chai, Nicolas Blanchemain, Gregory Stoclet, Frederic Cazaux, Séverine Bellayer, Stephanie Degoutin

► To cite this version:

Malo Dufay, Maude Jimenez, Mathilde Casetta, Feng Chai, Nicolas Blanchemain, et al.. Pcl covered pp meshes plasma-grafted by sulfonated monomer for the prevention of postoperative abdominal adhesions. *Materials Today Communications*, 2021, *Materials Today Communications*, 26, 10.1016/j.mtcomm.2020.101968 . hal-03986072

HAL Id: hal-03986072

<https://hal.univ-lille.fr/hal-03986072v1>

Submitted on 22 Mar 2023

HAL is a multi-disciplinary open access archive for the deposit and dissemination of scientific research documents, whether they are published or not. The documents may come from teaching and research institutions in France or abroad, or from public or private research centers.

L'archive ouverte pluridisciplinaire **HAL**, est destinée au dépôt et à la diffusion de documents scientifiques de niveau recherche, publiés ou non, émanant des établissements d'enseignement et de recherche français ou étrangers, des laboratoires publics ou privés.



Distributed under a Creative Commons Attribution - NonCommercial 4.0 International License

PCL covered PP meshes plasma-grafted by sulfonated monomer for the prevention of postoperative abdominal adhesions

*Malo Dufay¹, Maude Jimenez¹, Mathilde Casetta¹, Feng Chai², Nicolas Blanchemain², Grégory Stoclet¹,
Frédéric Cazaux¹, Séverine Bellayer¹, Stéphanie Degoutin^{*1}*

*stephanie.degoutin@univ-lille.fr

¹Univ. Lille, CNRS, INRAE, Centrale Lille, UMR 8207 - UMET - Unité Matériaux et Transformations, F-59000 Lille, France

²Univ. Lille, Inserm, CHU Lille, U1008, Controlled Drug Delivery Systems and Biomaterials, F-59000 Lille, France

Abstract

Abdominal hernia reparation constitutes the second surgical operation in the world with more than 20 million cases per year. However, in more than 50% of all intra-abdominal operations, postoperative adhesions occur and result in important pain for patients. These adhesions take place after excessive deposition of fibrin between peritoneum and organs within the 7 days after the operation which occurs during the coagulation cascade. For this reason, therapeutic solutions are required to both prevent adhesion and limit the need for a second surgical step. Numerous techniques were described in the past few decades to design biomedical textile implants and, among them, electrospinning shows great interest due to the porous and nanometer diameter range structure of the obtained fibers. In parallel, cold plasma treatment can be used to activate and graft their surface with functional molecules, exhibiting for example

antibacterial or anticoagulant properties. This work aims at functionalizing, biodegradable polycaprolactone (PCL) electrospun nanofibers covering polypropylene meshes (PPM) with 2-acrylamido-2-methylpropane sulfonic acid (AMPS) through cold plasma induced graft copolymerization. AMPS was chosen as it contains heparin-like segments, leading potentially to similar anticoagulant effect. First, electrospinning of PCL was optimized by varying process, solution and environmental parameters and allowed to select a solution of 12% of PCL in formic/acetic acid mixture. The graft-copolymerization of AMPS was then optimized in terms of power and time of plasma treatment, as well as solution concentration, using experimental design, in order to obtain nanofibers rich in SO₃H groups at their surface. At each step of the process, the material was thoroughly characterized proving the presence of AMPS onto the surface of the nanofibers. The cytocompatibility and anticoagulant properties, evaluated after sterilization, are promising for an anti-adhesive application of these nanofibrous mats with no release of cytotoxic compound.

Keywords: Electrospinning, cold plasma, surface modification, anticoagulant, abdominal repair

I. Introduction

Prevention of postoperative adhesions is one of the most important challenges in intra-abdominal surgery. In inguinal hernia treatment, the surgical procedure consists in depositing a mesh inside the hernia site in order to bring sufficient mechanical resistance and prevent recurrence of the hernia. After surgery, the healing process leads to the coagulation cascade and therefore the formation of fibrin. However, even if no fibrinolysis occurs seven days after the surgery, postoperative adhesions may appear between the peritoneum and the abdominal layer. These postoperative side effects occur in more than 55% of intra-abdominal operations and cause immediate chronic pain to the patients [1]. Two main strategies are currently developed in order to prevent postoperative adhesions: use of immunomodulatory molecules and deposition of mechanical barriers [2]. Regarding the concept of immunomodulation, several studies

deal with the use of interleukins (IL-1, 6 or 10) or also of antibodies (TGF- β_1 or TNF- α) as immunosuppressors. Results show good prevention of adhesion formation on rat model. However, all immunosuppressors are not able to limit the formation of adhesions area, as in the case of cyclosporin [3]. As far as we know, no study reveals that immunomodulatory agents show acceptable benefic/risk ratio in adhesion prevention on human model. In terms of mechanical barriers for antiadhesive applications, many investigations were carried out and therapeutic solutions were developed such as Intergel[®] [4], Seprafilm[®] [5] or SprayGel[®] [6] among others [7]. However, all these prevention systems require an additional step (deposition of film or gel) during the treatment of intra-abdominal surgeries. In this context, our strategy is to develop an abdominal implant covered with a biodegradable and bioactive layer, providing mechanical resistance for long-term healing and an anti-adhesive property to prevent postoperative adhesion. As mentioned previously, adhesions result from an excess of fibrin and depend on the coagulation cascade. In this sense, our hypothesis is based on the reduction of the coagulation cascade, leading hopefully to a decrease of adhesions formation, and the anticoagulant property is thus the targeted bioactive property for these implants.

Biodegradable polymers such as poly(lactic acid) (PLA) [8], poly(lactic-co-glycolic acid) (PLGA) [9] or polycaprolactone (PCL) [10] are mainly used as biodegradable scaffolds [11] due to their variable biodegradation rates and their excellent biocompatibility. As demonstrated by literature studies, electrospinning of biodegradable polymers has gained great interest in the past few decades, particularly due to the high porosity and high surface to volume ratio of the electrospun nanofibrous mats. The previously mentioned biodegradable polymers can be electrospun directly on a polypropylene mesh (PPM), and this approach is already used for repairing the inguinal hernia [12]. However, these polymers do not exhibit any bioactive property (anti-infection, anti-coagulant, etc.). Therefore, it is necessary to functionalize these polymeric nanofibers cover layer through an adequate surface treatment technique.

Cold plasma is known to be an efficient, ecofriendly and cost-effective surface treatment technique for polymeric materials as it often leads to an increase in hydrophilicity and to the modification of the intimal

physicochemical properties of the treated surface [13,14]. In particular, cold plasma treatment of polymer nanofibers has recently attracted increased attention [15]; almost half of the literature on this topic focuses on biodegradable polymers, and more precisely, on PCL or PLA [16,17]. In general, the increase in hydrophilicity [18] or hydrophobicity [19], the improvement of biocompatibility [16] or the addition of bioactivity[20] to the nanofibrous mats is targeted when applying cold plasma treatment. Different strategies are proposed such as polymer grafting [21,22], molecular grafting [23,24] or plasma-polymerization [16,20].

In this study, low pressure cold plasma treatment was used in order to functionalize PPM covered by PCL electrospun nanofibers with a sulfonated monomer. This functionalization was carried out in four steps: (I) argon cold plasma activation; (II) immersion in monomer solution; (III) padding and (IV) cold plasma graft-copolymerization of the monomer onto the surface of the nanofibers. First, acrylic acid grafting was used as a reference in order to prove the feasibility of the concept. Then, the grafting of 2-acrylamido-2-methylpropane sulfonic acid (AMPS) (as anticoagulant monomer) was optimized thanks to an experimental design. After sterilization, biological properties, such as cytocompatibility and anticoagulant activity, were assessed for optimized grafted samples.

II. Materials and methods

1. Materials

Polycaprolactone (PCL) (average $M_n \sim 80,000 \text{ g}\cdot\text{mol}^{-1}$), 2-acrylamido-2-methyl-1-propanesulfonic acid (AMPS), formic acid (95-97%), chloroform (CHCl_3), dichloromethane (DCM) and dimethylformamide (DMF) were purchased from Aldrich Chemicals (Saint Quentin Fallavier, France). Acrylic acid (AA) (99.5%) was purchased from Acros Organics (Illkirch, France) and glacial acetic acid (>99.8%) from Honeywell (Seelze, Germany). All these compounds were used without any further purification. Polypropylene meshes (PPM) (porosity of $73 \pm 1\%$, thickness of $0.25 \pm 0.13 \text{ mm}$ and mass per unit area of $32 \pm 4 \text{ g/m}^2$) were kindly provided by Cousin Biotech (Wervicq-Sud, France) and were washed by soxhlet extraction (ethanol, water and ethanol successively).

2. Methods

2.1. Electrospinning of PCL

PCL at different concentrations (7 to 12wt%) was added to 10 mL of formic acid/acetic acid mixture in various proportions (1:9 to 5:5 v/v) and solutions were stirred for 6 h to ensure homogeneity. The solution was injected in a needle of ~~0.723~~ 0.514 mm (21-G) inner diameter *via* a 10 mL polypropylene syringe at a controlled flow rate (between 0.5 and 1.5 mL.h⁻¹). All solutions were electrospun thanks to a homemade electrospinning apparatus and nanofibers were deposited on a rotating drum collector covered by PPM ~~tapped on~~ an aluminum foil ~~and the PPM~~. The distance between the needle and the collector was fixed at 20 cm and the voltage was set between 13 and 16 kV depending on solution and environmental conditions thanks to high voltage supplier. Electrospinning process was performed on both sides of the PPM in order to enhance the adhesion of the nanofibers and the mesh. **In that purpose, a first electrospinning step was carried out onto PPM and then, the obtained membrane was flipped and a second electrospinning step was carried out onto the other face.** Humidity and temperature were not controlled during electrospinning but were measured in order to evaluate the effect of these parameters.

2.2. Functionalization of PCL electrospun fibers by cold plasma

Samples (3 x 3 cm²) were cut from membranes composed of two layers of PCL electrospun fibers and one inner layer of PPM. Samples were then placed **(being held with a clamp)** in a low-pressure plasma chamber (Europlasma apparatus CDI1200-400 COMBI MC, Radio Frequency Generator Dressler, 13.56 MHz) and the pressure was set down to 50 mbar. Argon flow rate, power and plasma duration were varied in order to modify the surface wettability of the membranes. At the end of the treatment, the plasma chamber was filled with dry and de-oiled air for 30 seconds. Samples were then immersed in the monomer solution, either AA/water or AMPS/water in different proportions, for 5 seconds and, after a padding process, were placed once again in the plasma chamber. As for the first plasma treatment, the three different parameters were varied in order to optimize the graft-copolymerization of the monomer onto the

surface of the membranes. An experimental design was set up to determine the optimized parameters leading to a homogeneous and reproducible grafting. Finally, samples were washed in a 200 mL distilled water bath and dried under vacuum in an oven at 40°C for 8 h. The entire procedure is described in **Figure 1**. **It is important to note that both sides of the samples were treated identically, leading to similar grafting, and so properties, of each side of the scaffold.**

Figure 1: Summary diagram of the entire functionalization process

2.3. Experimental design of AMPS grafting

To determine the plasma treatment conditions leading to the optimum AMPS grafting, experimental design was implemented using response surface methodology (RSM). The influence of three main process parameters was studied: the power and duration of plasma treatment and the AMPS concentration used for the grafting step. A central composite design (CCD), consisting of 17 experiments was performed and was composed as follows:

- the first 8 experiments correspond to a 2^k full factorial design, k being the number of studied variables (3 in this experimental design),
- the following 6 experiments ($2 \times k$) are axial points at a distance of $\alpha=1.68$ from the design center,
- and finally, 3 experiments being replicates of the center point.

Experiments were conducted randomly to provide protection against the extraneous factors, which could affect the measured response. For statistical calculations, the variables U_i were coded as X_i according to **(Equation 1)**:

$$X_i = \frac{(U_i - U_0)}{\Delta U}$$

(Equation 1)

where X_i is the dimensionless coded value of U_i variable, U_0 represents the value of U_i at the center point and ΔU is the step change.

The experimental values associated to the coded levels of the different variables are given in

Table 1.

The quadratic model for predicting the optimal conditions was expressed according to **(Equation 2)**:

$$Y = \beta_0 + \sum_{i=1}^n \beta_i X_i + \sum_{i<j}^n \beta_{ij} X_i X_j + \sum_{i=1}^n \beta_{ii} X_i^2$$

(Equation 2)

where Y is the considered response variable, β_0 is the value of the fitted response at the center point, β_i , β_{ii} and β_{ij} correspond to the linear, quadratic and interaction terms respectively.

Table 1: Coded and real values of experimental parameters used for the CCD

Coded variables	Parameter	Levels				
		$-\alpha$	-1	0	+1	$+\alpha$
X_1	U ₁ , plasma power (W)	50	70	100	130	150
X_2	U ₂ , time of plasma treatment (s)	60	80	100	140	160
X_3	U ₃ , AMPS concentration (g, water qsp 10g)	1	1.4	2	2.6	3

2.4. Scanning electron microscopy (SEM) and energy-dispersive X-ray spectroscopy (EDX)

The morphology and diameters of the nanofibers were analyzed before and after each processing step using a SEM Flexsem 1000 Hitachi with an accelerating voltage of 5 kV and an emission current of 10 μ A. EDX analysis was carried out with the same apparatus in the same conditions. All the samples were carbon coated with a 20 nm layer. The average diameter of the nanofibers was evaluated by ImageJ software, taking into account the metallization thickness.

2.5. Water contact angle analysis

The change in the surface wettability of the nanofibers after plasma treatment was determined by measuring the evolution of the contact angle of a water droplet (3 μ L) deposited directly onto the sample

and was analyzed thanks to a Minitec Krüss DSA 100 goniometer. The temperature during the analysis was $20 \pm 1^\circ\text{C}$ and all measurements were done in triplicate.

2.6. Toluidine blue O (TBO) assays

In the case of acrylic acid grafting, the amount of carboxylic groups onto the surface of the nanofibers (expressed in μmol of COOH groups per cm^2 of sample) was determined thanks to a colorimetric assay, already described in a previous paper of the laboratory [25], allowing to quantify the grafting efficiency. Briefly, grafted and ungrafted samples were immersed in 20 mL of a TBO solution and stabilized at pH 10 for 4h under stirring at ambient temperature. Then, samples were rinsed in NaOH solution (0.1 M) in order to remove uncomplexed TBO and membranes were immersed in an acetic acid solution (50%) in order to allow the desorption of TBO. Finally, the solutions obtained were analyzed by UV spectrophotometry (UV-1800 Shimadzu spectrometer) at 634 nm. The amount of adsorbed TBO was finally correlated to the grafting amount of carboxylic functions according to Beer Lambert law.

2.7. *In vitro* biological assays

All *in vitro* experiments were performed in triplicate on gamma-sterilized samples (40 kGy) and are described hereafter. Mean cell proliferation and coagulation results were analyzed by ANOVA, and a significant difference was considered for $p < 0.05$.

2.7.1. *In vitro* cell viability by indirect contact

PPM disks of 11 mm diameter, covered by PCL nanofibers, functionalized or not, were extracted in complete culture medium according to ISO 10993-5 ($6 \text{ cm}^2/\text{mL}$) for 24h and 72h at 37°C under 80 rpm agitation. Simultaneously, NIH/3T3 fibroblast cells (ATCC[®] CRL-1658) were seeded in 96 well tissue culture plate filled with 100 μL of complete culture medium at 4.0×10^3 cells per well. After 24h, the extraction medium was filtered through 0.22 μm sterile filters (PB Acrodisc[®]; PALL, France) for sterilization. After culture medium removal from the tissue culture plate, sterile extraction medium was put into contact with NIH/3T3 fibroblasts monolayer for 72h at 37°C . After incubation, cellular medium

was removed and replaced by a solution composed of 180 μL of complete culture medium and 20 μL of AlamarBlue[®] for 2h in an incubator protected from light. Then, 150 μL of this solution were withdrawn to analyze the fluorescence intensity at a wavelength of 590 nm (emission) on a TwinkleTMLB 970 fluorometer. Obtained results were normalized to the negative controls (the complete culture medium).

2.7.2. *In vitro* cell viability by direct contact

Cell viability assessments by direct contact were performed in accordance with a previous study of the laboratory [26]. Briefly, PPM disks covered by PCL nanofibers, functionalized or not, were placed in 48-well plate and cells (4000 cells \times cm^{-2}) were gently seeded onto these disks and incubated for 3 and 6 days without any modification of the culture medium. Similarly to indirect contact assays, the culture medium was then replaced by a new culture medium containing AlamarBlue[®]. After 2h of incubation protected from light, these media were analyzed by fluorometry as for indirect contact.

2.7.3. *In vitro* anticoagulation assays

According to ISO 10993-4 standard, PPM disks of 11 mm diameter, covered by functionalized or non-functionalized nanofibers, were immersed in complete blood, donated by healthy volunteer young adult *via* citrated tubes. This complete blood, in contact with the different samples, was incubated at 37°C for 30 minutes, shaken at 80 rpm and then centrifuged at 2,500 g at 14°C for 15 minutes in order to separate the blood cells from poor platelet plasma (PPP). Three coagulation tests were then carried out with collected PPP: (1) Activated partial thromboplastin time (APTT) test, in which 50 μL of PPP were incubated at 37°C for 1 minute, mixed with 50 μL of TriniCLOT[™] aPTT HS, Tcoag[®] (TCA) reactant, incubated for 5 minutes and finally coagulation time was measured after addition of 100 μL of CaCl_2 (0.025 $\text{mol}\cdot\text{mL}^{-1}$); (2) Prothrombin time (PT) test, in which 100 μL of PPP were incubated at 37°C for 2 minutes, mixed with 200 μL of NEOPLATINE[®] (Diagnostica Stago, Inc.) (incubated for 10 minutes at 37°C) and the coagulation time was then measured; and (3) anti-Xa test, following the manufacturer protocol (HYPHEN BioMed) [27]. For each experiment, 1, 2 and 3 disks of each sample were tested independently in order to determine the influence of active surface area on the anticoagulant effect.

2.7.4. *In vitro* hemolysis assays

PPM disks of 11 mm diameter, covered by nanofibers, functionalized by AMPS or not, were immersed in 1 mL of complete human blood from healthy donor. Samples were incubated at 37°C for 30 min, shaken at 80 rpm and the disks were then removed. Triton X-100 (Thermo Scientific™) in 0.9% (w/v) NaCl solution was used as positive control (100% lysis) and 0.9% (w/v) NaCl solution was used as negative control (0% lysis). 0.9% (w/v) NaCl solution was added to each tube of blood with samples in order to obtain a blood concentration of 5 mg.mL⁻¹. Finally, the blood solutions were centrifugated at 2,500 g for 10 min, and the supernatants were analyzed by UV-vis spectroscopy at 540 nm in order to detect hemoglobin.

III. Results and discussion

1. *Electrospinning of PCL on PPM*

Figure 2: SEM images of nanofibrous membranes with different PCL concentrations and formic/acetic acid ratios (Experimental conditions: RH = 30%, T = 25°C, V = 13- 16 kV, flow rate = 0.5 mL.h⁻¹, distance tip to collector = 20 cm).

Electrospinning parameters of PCL were optimized by focusing first on the solvent nature. In the literature, organic solvents are mainly used for PCL electrospinning. First, PCL was electrospun in CHCl₃ and in a mixture of DCM/DMF (4/6) at concentrations of 8% and 12% respectively. Specific structures such as porous nanofibers with high diameters and dispersion were observed. This was already described in the literature as a consequence of the relative humidity and temperature [28]. Indeed, in our case, the relative humidity varied between 30 and 50% and the temperature between 19 and 21°C. In these conditions, some water droplets may percolate inside the jet during solvent evaporation and create porous nanofiber structures. Besides, the high humidity level may inhibit solvent evaporation during the time of flight of the jet and cause a high dispersion of the nanofibers diameters. Moreover, organic solvents exhibit some toxicity and should be avoided in the case of biomedical applications. As an alternative to organic solvents, Liverani *et al.* studied the use of acidic solvents for the electrospinning of PCL [29]. A

mixture of acetic acid and formic acid was thus tested. **Figure 2** shows an increase in the amount and the size of beads with the decrease in formic acid concentration as well as with the decrease of PCL concentration. These results prove that the adequate combination of concentrations leads to the formation of defect-free nanofibers. The following concentrations were considered for further investigations: 12 wt% PCL in 5/5 formic/acetic acid. Besides solution parameters, process and environmental conditions were optimized in order to obtain defect-free nanofibrous mats. In this sense, the two parameters significantly affecting the morphology of the mats were relative humidity (RH) and flow rate. SEM pictures of the nanofibers at various RH levels or flow rates are given in **Figure 3**. It is shown that an increase in humidity during electrospinning process leads to the formation of a film with fewer nanofibers. This phenomenon is due to the fact that, under very wet conditions, solvent cannot evaporate correctly and nanofibers deposited on the collector are not totally dry. **Indeed, if there is too much humidity in the electrospinning chamber, the acid raises the vapor pressure faster than for low humidity and thus, there is too much remaining solvent in the nanofibers at the deposition instant which causes the partial solubilization of these fibers.** In parallel, an increase of the flow rate could be balanced by an increase of the voltage. However, for a too high voltage, the jet is less stable, and some beads are created, as can be seen in the lower part of **Figure 3**.

Figure 3: SEM images of the morphology of PCL nanofibers depending on relative humidity and flow rate. For each flow rate the humidity was about 30 ± 2 %, and for each humidity rate, the flow rate was fixed at 0,5 mL/h.

Hence, for all experiments described thereafter, the PCL mats are obtained by electrospinning onto the PPM with the following conditions: 12%wt of PCL in formic/acetic acid (5:5) at 1 mL/h and with a RH lower than 40% and a temperature between 20 and 25°C.

2. Cold plasma treatment of PCL covered PPM

2.1. Hydrophilicity enhancement

The first cold plasma treatment is carried out in order to increase the hydrophilicity of PCL nanofibers. Indeed, as observed in **Figure 4A**, the water contact angle (WCA) of untreated PCL

nanofibers is $138 \pm 2^\circ$, showing that electrospun mats are highly hydrophobic. Several conditions of plasma treatment were carried out on nanofibrous membranes in order to determine the effect on the morphology and the hydrophilicity of mats. The following parameters were varied: the duration, the power and the argon flow rate of plasma treatment. The first observation is that the morphology and the diameter of the nanofibers (**Figure 4B and C**) are not significantly affected by the plasma treatment, whatever the conditions (**Figure 4D**). Additionally, WCA measurements were performed in order to quantify the increase of hydrophilicity of the nanofibers. It is important to note that all the plasma treated nanofibrous mats adsorb, more or less quickly, the water drop. This phenomenon is due to the high porosity of the samples, which, combined with the increase in hydrophilicity, leads to the penetration of the water drop inside the mats. Moreover, the cold plasma treatment is known to act on the porosity of the treated materials and so, in our case, allows a diffusion of the water directly into the nanofibers. Thus, the increase in hydrophilicity of the nanofibers mats was not measurable by WCA. However, the time of drop adsorption depends on the plasma conditions. In particular, the modification of the plasma treatment duration leads to an important change in the adsorption time of the drop. As shown in **Figure 5**, if the plasma treatment time is longer than 200 s (for a plasma power around 100 W and a flow rate of argon of 15 sccm (standard cubic centimeter per minute)), the water drop is adsorbed instantly. **The hydrophilicity of this kind of plasma treatment was not stable in the time. Indeed, after few hours, surface functions created by plasma treatment started to reorganize and the hydrophilicity of the samples decreased rapidly. After one day, the surface of the samples exhibits equivalent hydrophobicity to the untreated samples.**

Figure 4: A: Image of WCA on PCL nanofibers before plasma treatment; B: SEM image of untreated nanofibers; C: SEM image of plasma treated nanofibers in conditions 9; D: Evolution of nanofibers diameter depending on cold plasma conditions given in the table (red: lower conditions; black: middle conditions and green: higher conditions)

Figure 5: Influence of plasma treatment time of nanofibrous mats on the adsorption time of the water drop (power = 100 W and flow rate of argon = 15 sccm)

2.2. Acrylic acid grafting

The functionalization of PCL nanofibers was first carried out with acrylic acid as reference. Indeed, acrylic acid is known to well graft-copolymerize by cold plasma [30]. The procedure was carried out in three steps: firstly, nanofibers were treated by cold plasma in the conditions determined previously ($P = 100 \text{ W}$; $t = 200 \text{ s}$ and flow rate = 15 sccm). Then, the plasma treated nanofibrous mats were immersed in a solution of acrylic acid (AA) in water (20% v/v) for 5 seconds followed by a padding step in order to remove the excess of AA. Finally, the second plasma treatment was performed in order to graft and copolymerize AA onto the nanofibers. **Figure 6** shows the SEM images of the morphology of the nanofibers after each step of the process. It can be seen that the nanofibers diameter is strongly increased after the grafting process, even after a washing step in water (**Figure 6C**). In order to understand which step of the procedure is mainly responsible for this phenomenon, additional investigations were carried out. First, the washing time was raised from 3 to 48 hours and no modification of the morphology of the nanofibers was observed, meaning that the non-grafted AA was totally removed after 3 hours of washing. In parallel, the whole process was performed with water instead of acrylic acid to determine if the increase in diameter is due to AA or to the process. The nanofibers' morphology was studied after each step and results are presented in **Figure 7**. An important swelling of the nanofibers is observed after the first cold plasma treatment followed by water immersion (**Figure 7B**) and for the whole process in water (**Figure 7D**). However, a much lower swelling is observed for the nanofibers immersed in water (**Figure 7A**) and for the samples immersed in water followed by the second plasma process (**Figure 7C**) i.e. for experimental conditions without the first cold plasma treatment.

Figure 6: SEM images of the nanofibers after different steps of the grafting process (with acrylic acid). A: after first cold plasma treatment; B: after first cold plasma, immersion in AA and second cold plasma treatment; C: after first cold plasma, immersion in AA, second cold plasma treatment and 3h washing in water.

Figure 7: SEM images of nanofibers after each step of the process in water (A: Immersion in water without first and second plasma treatment; B: immersion after first plasma treatment; C: immersion followed by second plasma treatment and D: whole process in water).

These results allow to conclude that the nanofibers swelling is not due to the use of AA or to the grafting step. On the contrary, the first plasma treatment has a decisive role in the nanofibers swelling and this phenomenon can be explained by the increase in absorption properties, as demonstrated previously in **Figure 5**. Indeed, plasma treatment leads to an increase in nanofibers ~~porosity~~ **roughness and degradation**, which allows water penetration and causes a swelling of the fibers. **It is also important to note that, no swelling of the nanofibers was observed between the Figure 7A and Figure 7C which means that the second plasma treatment did not lead to a swelling of the fibers. However, an increase of the nanofibers diameter between Figure 7B and Figure 7D can be observed, thus implying that the second plasma has an effect on the swelling of the nanofibers. An hypothesis is that the first plasma treatment weakened the nanofibers and lead to the permeation to the water while the second plasma cause a second weakening of fibers and water inside fibers generates a higher swelling.** Therefore, the first plasma treatment conditions must be adjusted in order to increase the nanofibers hydrophilicity while preventing nanofibers swelling. The following set of cold plasma parameters for the first treatment was used: P = 50 W, t = 80 s, flow rate = 15 sccm. Thus, all the process was then carried out in acrylic acid solution (2/8 AA:water) and the grafting of AA onto PCL nanofibers was then characterized by colorimetric TBO assay (**Figure 8**).

Figure 8: SEM images of nanofibers before (A) and after (B) the grafting of acrylic acid by plasma process and amount of COOH groups at the nanofibers surface determined through TBO assay

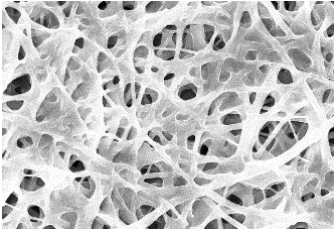
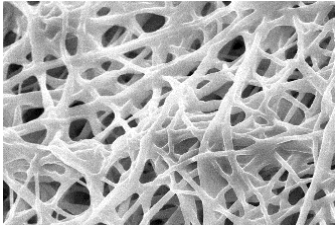
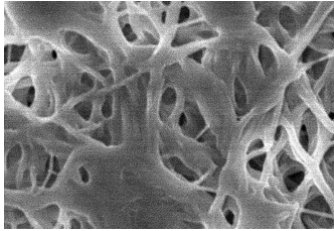
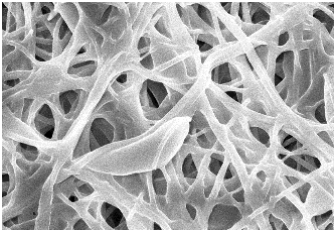
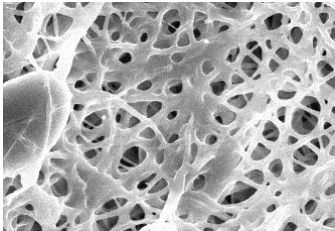
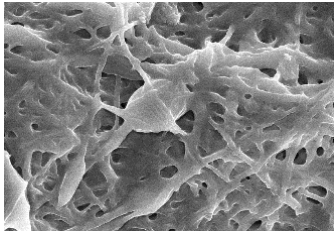
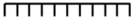
TBO adsorption results demonstrate that acrylic acid is successfully grafted on PCL nanofibers, even after the washing step. Moreover, the washing time does not affect significantly the amount of COOH functions onto the surface of the nanofibers, and therefore the grafting efficiency of acrylic acid. However, a minimum washing time (1h) is required to remove ungrafted acrylic acid, otherwise, a film (as on **Figure 6B**) is observed at the surface of the sample.

All these results **showed the influence of each step of the process on the grafting of acrylic acid onto PCL nanofibers.** The feasibility of the plasma grafting onto PCL nanofibers having been demonstrated, the protocol must now be adapted to the grafting of AMPS onto nanofibers.

2.3. Optimization of AMPS grafting

Some preliminary experiments were carried out before the optimization of AMPS grafting through experimental design methodology. First, the cold plasma treatment for surface activation was optimized in order to determine its effect on the resulting nanofibers morphology. In this sense, two sets of cold plasma conditions were tested for this activation step: P_{low} ($P = 50$ W, $t = 80$ s, flow rate = 15 sccm) and P_{high} ($P = 90$ W, $t = 120$ s, flow rate = 15 sccm). Treated membranes were then immersed in AMPS solution whose concentration was varied (AMPS/water 1:9, 2:8 and 3:7) to determine the effect on nanofibers morphology. Finally, impregnated samples were submitted to the second cold plasma treatment in constant conditions ($P = 50$ W, $t = 80$ s, flow rate = 15 sccm) in order to study only the effect of the first plasma treatment conditions. Results given in **Table 2** show that, as for acrylic acid, an increase in plasma power and duration and an increase in AMPS solution concentration lead to an increase in nanofibers swelling.

Table 2: Nanofibers morphology according to the first cold plasma treatment conditions and according to the AMPS solution concentration

	AMPS/water 1:9	AMPS/water 2:8	AMPS/water 3:7
P_{low}			
P_{high}			 3 μm 

Thus, the P_{low} first plasma treatment conditions were chosen in order to maintain the nanofibrous structure. In addition, X-ray spectroscopy was performed on the plasma sample treated with AMPS and the EDX spectrum (**Figure 9**) exhibits a peak at 2.15 keV, corresponding to sulfur, confirming the presence of AMPS onto the nanofibres (this peak was not observed for the untreated sample).

Figure 9: EDX spectrum of AMPS plasma grafted PCL nanofibers

These preliminary results show that AMPS is properly grafted onto the nanofibrous membrane even after a 1 h washing step. However, the second plasma treatment conditions, as well as the concentration of AMPS in the immersion solution must be optimized in order to obtain the best morphology for the AMPS grafted sample. That is why surface response methodology was applied to the plasma grafting step.

The quality of AMPS grafting after the plasma treatment has been taken as the response in the composite design. To quantify precisely this criterion, the nanofibers morphology after grafting was analyzed by SEM and a classification from 0 (homogeneous distribution of polymer coating onto the nanofibers without aggregates) to 4 (samples without grafting) was established (**Figure 10**).

The experimental conditions (U_i) applied for the 17 experiments and the experimental results obtained for the grafting (Y) are shown in **Table 3**. For each experiment, the response corresponds to the average of 3 measurements.

Figure 10: Classification of AMPS grafting quality

Table 3: CCD in coded and real values with the corresponding experimental results obtained in terms of grafting

Experiments	X1	X2	X3	U1	U2	U3	Grafting quality (Y)
1	-1	-1	-1	70	80	1.4	0.17
2	+1	-1	-1	130	80	1.4	0.33
3	-1	+1	-1	70	140	1.4	1.33
4	+1	+1	-1	130	140	1.4	1.5
5	-1	-1	+1	70	80	2.6	1.33
6	+1	-1	+1	130	80	2.6	1
7	-1	+1	+1	70	140	2.6	1

8	+1	+1	+1	130	140	2.6	1
9	- α	0	0	50	110	2	0.17
10	+ α	0	0	150	110	2	0.25
11	0	- α	0	100	60	2	0.67
12	0	+ α	0	100	160	2	0.67
13	0	0	- α	100	110	1	0.33
14	0	0	+ α	100	110	3	1
15	0	0	0	100	110	2	0.63
16	0	0	0	100	110	2	0.63
17	0	0	0	100	110	2	0.63

The statistical significance of the main, quadratic and interaction effects of the variables was determined by analysis of variance (ANOVA) and a multiple regression analysis was performed to fit the experimental data to the second-order polynomial equation ((**Equation 2**)).

The determination coefficients R^2 and R^2_{Adjusted} describe respectively the fraction of variation of the response explained by the model and the fraction of variation of the response explained by the model adjusted for degrees of freedom. The coefficient of prediction, Q^2 , describes the fraction of variation of the response that can be predicted by the model.

When the 17 experiments are considered, the determination coefficient is low ($R^2 = 69\%$). To improve the statistical significance of the model, experiments 11 and 12 were removed from the composite design as they did not fit well with the model. These experiments correspond respectively to the shortest (60 s) and longest (160 s) processing times, suggesting that the grafting efficiency is strongly modified when the time of plasma treatment is significantly reduced or extended. After the removal of these two experiments, R^2 is now equal to 98.8%, indicating that less than 2% of the total variation is not explained by the model. The value of the adjusted determination coefficient is also high ($R^2_{\text{Adjusted}} = 96.6\%$), showing a high significance of the model. Moreover, the quality of the grafting is well predicted by the model with a coefficient of prediction (Q^2) equal to 80.3%.

After checking the reliability of the model, the significance of the different model terms can be discussed. Their values are listed in **Table 4**.

Table 4: Main, quadratic and interactions coefficients of the model determined with Modde7.0

Coefficients	Grafting quality
β_0	0.63
β_1	0.010
β_2	0.25
β_3	0.156
β_{11}	-0.151
β_{22}	0.466
β_{33}	0.013
β_{12}	0.043
β_{13}	-0.083
β_{23}	-0.333

Among the different main and quadratic effects, β_2 and β_{22} terms have the highest value. Thus, within the ranges tested, the grafting is strongly affected by a change in the duration of the plasma treatment (parameter X2). Moreover, these terms being positive, it means that an increase in plasma treatment duration leads to an increase in the response. As the value of the grafting quality (Y) has to be as close to 0 as possible, the plasma treatment duration must be minimized. However, it was shown previously that the duration of this treatment should be higher than 80 s to fulfill the statistical criteria. Thus, the response surface was plotted for a time ranging from 80 to 140 s (**Figure 11**). This figure allows confirming that the lowest responses are obtained when the time is low, more precisely between 80 and 100 s. Thus, this parameter was set at 90 s.

Figure 11: A: Contour plot showing the evolution of the grafting as a function of AMPS concentration and plasma treatment time for a constant power of 90 W; B: Contour plot showing the evolution of the grafting as a function of AMPS concentration and plasma treatment power for a constant time of 90 s

Then, the third variable corresponding to the monomer concentration is characterized by an important main coefficient (β_3) and also a strong interaction with plasma duration (high β_{23} in absolute value). Thus, this parameter has to be considered for the grafting optimization. **Figure 11A** shows that the lowest results are obtained for low concentrations of AMPS. More precisely it can be observed that

responses lower than 0.2 can be obtained for an AMPS concentration ranging from 1 to 1.2, combined with a treatment time between 80 and 100 s. Thus, AMPS concentration was set at 1.1.

Finally, the main coefficient associated to the first variable (i.e. β_1) as well as the interaction coefficients containing parameter X1 (i.e. β_{12} and β_{13}) are very low, meaning that the grafting is very little affected by a change in the plasma power. **Figure 11B** allows confirming this statement, showing that for a given AMPS concentration and a given time of plasma treatment, the response remains almost constant whatever the plasma power. In the previously selected conditions (plasma duration of 90 s and AMPS concentration of 1.1), the response is always lower than 0.15. So, for economical and practical reasons, the power has been set at 90 W.

Thus, the conditions allowing to optimize the grafting were determined as follows: 90 s of plasma treatment at 90 W, with an AMPS concentration of 1.1. In these conditions, the value of the grafting predicted by the model is around 0.08. The morphology of the nanofibers after grafting in the optimized conditions was analyzed by SEM (**Figure 12**). The membrane exhibits a nanofibrous structure without aggregates allowing validating the experimental design method.

Then the biological properties of the grafted samples in the optimized conditions were studied. In parallel, maximal conditions of grafting (P = 150 W, T = 160 s, conc. = 3/7 AMPS:water, w/v) were also applied in order to compare the biological properties obtained with the two sets of parameters.

Figure 12: SEM image of the grafted sample in the optimized conditions (90 W, 90 s, 1.1 g AMPS)

3. Biological assessments

3.1. Cellular viability test

The untreated and plasma grafted samples in optimal and maximal conditions were evaluated by indirect contact cellular viability test on NIH/3T3 cells (**Figure 13A**). First of all, these results show that all the treated and untreated samples do not release any cytotoxic compound after 24 h and 72 h extraction. However, in order to prove the cytocompatibility of PPM-PCL grafted materials, direct contact

assay is assessed. NIH/3T3 cells were directly put into contact with the membranes, for 3 and 6 days, and results are presented on **Figure 13B**.

The untreated sample (PP-PCL) shows a proliferation of $66 \pm 8\%$ after 3 days of culture compared to the control (TCPS). However, the proliferation increases after 6 days of culture ($84 \pm 10\%$), that reveals a slightly more intense metabolic activity of the cells developed onto this sample. This lower proliferation could be explained by the hydrophobicity of PP-PCL highlighted previously (**Figure 4A**). After the functionalization process, the proliferation decreases to $55 \pm 10\%$ and $45 \pm 8\%$ after 3 days of culture for Optimal and Maximal conditions respectively. This decrease could be explained by the surface charge density (due to grafted functions), inducing a local pH reduction as already discussed in a previous paper[25]. In the same way as for PP-PCL sample, the proliferation increases after 6 days of testing, showing that the low proliferation is due to a delay in cell growth and not to a cytotoxic effect.

One of the requirements of the nanofibers covered PPM used for hernia-repair applications is to avoid the postoperative adhesions, occurring by excessive fibrin deposition within 7 days after surgery. In this sense, a limited cell proliferation on the membranes is clearly helpful to prevent the deposition of fibroblasts provided that any toxicity is observed, as evidenced here by the constant cell viability with time. Finally, another noticeable phenomenon is that cell viability for optimal samples is significantly higher than for maximal samples after 3 days of contact ($p < 0.05$). However, this tendency is not observed after 6 days of contact (no significant difference in ANOVA for $p < 0.05$). Thus, the selection of the best candidates for future *in vivo* studies is far from obvious if only cell viability results are considered.

*Figure 13: A: NIH3T3 cells viability after 24 and 72 h contact with cellular medium (control) or extraction medium of untreated PP-PCL or plasma grafted samples in optimal and maximal plasma conditions; B: NIH3T3 cells viability after 3 and 6 days contact with TCPS (control), PP-PCL, plasma grafted samples in optimal and maximal plasma conditions. * $p < 0.05$*

3.2.Coagulation test

In order to prove the efficiency of the AMPS grafting *via* its anticoagulant activity, the samples were tested through three *in vitro* assays in contact with whole blood. The coagulation time of blood was

evaluated by immersion of 1, 2 and 3 sample disks respectively, and the results are reported in **Figure 14**. As expected, similar behavior is observed for control (blood alone) and for blood-soaked PCL-PPM (reference as non-anticoagulant surfaces). Except for 1 disk of optimal treated samples, all other groups show anticoagulant activity with an average APTT longer than 40 s. Moreover, the increase in the number of disks (2 or 3 disks) of maximal or optimal conditions samples in the immersion medium leads to a higher anticoagulant activity (average APTT of around 65 s), comparable to that of 0.5 unit of heparin, without any significant difference between maximal and optimal conditions samples (if the same number of disks is considered) ($p > 0.05$). Interestingly, there is a significant difference in anticoagulant activity between 1 disk (760 mm² of active surface area) of optimal or maximal samples and 2 or 3 disks, suggesting a dose-dependent activity for the grafted surface. Finally, the results of hemolysis assays show that no significant absorbance peak relative to hemoglobin (540 nm) is observed on UV spectra for the samples, whatever the number of blood-soaked disks. These results are particularly promising to reach a good hemocompatibility of the grafted samples.

Overall, beyond the cytocompatibility and the hemocompatibility, these AMPS grafted nanofibres exhibit an interesting anticoagulant effect when a minimum grafted surface area is used. As described previously, cascade coagulation plays a key role in adhesion phenomenon, and so, by delaying the clotting cascade, adhesion could be efficiently limited. In this sense, these AMPS grafted PCL nanofibers are promising candidates for the limitation of postoperative adhesions for hernia repair.

*Figure 14: Coagulation time of healthy blood on TCPS (control) with or without 0.5 unit of heparin and on various numbers of disks of PPM covered by PCL nanofibers functionalized (optimal and maximal) or not (reference); 1 disk, 2 disks and 3 disks represent different surface area put into contact with blood (respectively 760, 1520 and 2280 mm²); * $p < 0.05$*

IV. Conclusions

In this study, polypropylene meshes used in the hernia treatment were covered by PCL nanofibers and then functionalized in order to provide anticoagulant and expected antiadhesive properties in order to avoid postoperative adhesions after intra-abdominal surgery. After the optimization of the PCL

electrospinning, acrylic acid was first successfully grafted on these meshes thanks to cold plasma treatment in order to prove the feasibility of the approach. Then the grafting of AMPS, a monomer possessing sulfonate groups expected to exhibit anticoagulant activity, was optimized through experimental design methodology. Whatever the conditions of treatment, and after sterilization, PPM meshes, treated or not, did not release any cytotoxic compound, and demonstrate sufficient cell viability in direct contact with cells. In terms of anticoagulant activity, AMPS grafted samples exhibit properties very similar to that of 0.5 unit of heparin if sufficient grafted surface area is used. All these results showed firstly that plasma treatment did not affect the anticoagulant activity of AMPS and also that the graft-copolymerization of this monomer on PCL nanofibers covered PPM leads to promising anticoagulant activity with an acceptable cytocompatibility with fibroblasts NIH3T3. Future work will concentrate on mechanical properties of samples and on degradation rate in order to select the best cold plasma treatment for inguinal hernia repair application. Then, studies will be focused on *in vivo* assays in order to prove the efficiency of these plasma treated nanofibers covered PPM on a rat model for the treatment of inguinal hernia to limit the postoperative adhesions.

Acknowledgments

The authors thank Agence Nationale de la Recherche (ANR JCJC CAPSPIN: ANR-17-CE09-0003-01) and Euramaterials competitiveness Cluster for supporting and funding this work. Thanks to Alexandre Ung (service Hémostase, Hospital Center University of Lille (CHU-Lille)) for help in blood coagulation test.

References

- [1] Postoperative Adhesion Development after Operative Laparoscopy: Evaluation at Early Second-Look Procedures**Presented in Part at the 46th Annual Meeting of The American Fertility Society, Washington D.C., October 15 to 18, 1990. *Fertil. Steril.* **1991**, 55 (4), 700–704. [https://doi.org/10.1016/S0015-0282\(16\)54233-2](https://doi.org/10.1016/S0015-0282(16)54233-2).
- [2] Rocca, A.; Aprea, G.; Surfaro, G.; Amato, M.; Giuliani, A.; Paccone, M.; Salzano, A.; Russo, A.; Tafuri, D.; Amato, B. Prevention and Treatment of Peritoneal Adhesions in Patients Affected by

- Vascular Diseases Following Surgery: A Review of the Literature. *Open Med. Wars. Pol.* **2016**, *11* (1), 106–114. <https://doi.org/10.1515/med-2016-0021>.
- [3] Cheong, Y. C.; Laird, S. M.; Li, T. C.; Shelton, J. B.; Ledger, W. L.; Cooke, I. D. Peritoneal Healing and Adhesion Formation/Reformation. *Hum. Reprod. Update* **2001**, *7* (6), 556–566. <https://doi.org/10.1093/humupd/7.6.556>.
- [4] Johns, D. B.; Keyport, G. M.; Hoehler, F.; diZerega, G. S.; Intergel Adhesion Prevention Study Group. Reduction of Postsurgical Adhesions with Intergel Adhesion Prevention Solution: A Multicenter Study of Safety and Efficacy after Conservative Gynecologic Surgery. *Fertil. Steril.* **2001**, *76* (3), 595–604. [https://doi.org/10.1016/s0015-0282\(01\)01954-9](https://doi.org/10.1016/s0015-0282(01)01954-9).
- [5] Becker, J. M.; Dayton, M. T.; Fazio, V. W.; Beck, D. E.; Stryker, S. J.; Wexner, S. D.; Wolff, B. G.; Roberts, P. L.; Smith, L. E.; Sweeney, S. A.; Moore, M. Prevention of Postoperative Abdominal Adhesions by a Sodium Hyaluronate-Based Bioresorbable Membrane: A Prospective, Randomized, Double-Blind Multicenter Study. *J. Am. Coll. Surg.* **1996**, *183* (4), 297–306.
- [6] Mettler, L.; Audebert, A.; Lehmann-Willenbrock, E.; Schive-Peterhansl, K.; Jacobs, V. R. A Randomized, Prospective, Controlled, Multicenter Clinical Trial of a Sprayable, Site-Specific Adhesion Barrier System in Patients Undergoing Myomectomy. *Fertil. Steril.* **2004**, *82* (2), 398–404. <https://doi.org/10.1016/j.fertnstert.2003.12.046>.
- [7] Kamel, R. M. Prevention of Postoperative Peritoneal Adhesions. *Eur. J. Obstet. Gynecol. Reprod. Biol.* **2010**, *150* (2), 111–118. <https://doi.org/10.1016/j.ejogrb.2010.02.003>.
- [8] Soundararajan, A.; Muralidhar R, J.; Dhandapani, R.; Radhakrishnan, J.; Manigandan, A.; Kalyanasundaram, S.; Sethuraman, S.; Subramanian, A. Surface Topography of Polylactic Acid Nanofibrous Mats: Influence on Blood Compatibility. *J. Mater. Sci. Mater. Med.* **2018**, *29* (9), 145. <https://doi.org/10.1007/s10856-018-6153-2>.
- [9] Gentile, P.; Chiono, V.; Carmagnola, I.; Hatton, P. V. An Overview of Poly(Lactic-Co-Glycolic) Acid (PLGA)-Based Biomaterials for Bone Tissue Engineering. *Int. J. Mol. Sci.* **2014**, *15* (3), 3640–3659. <https://doi.org/10.3390/ijms15033640>.
- [10] Mochane, M. J.; Motsoeneng, T. S.; Sadiku, E. R.; Mokhena, T. C.; Sefadi, J. S. Morphology and Properties of Electrospun PCL and Its Composites for Medical Applications: A Mini Review. *Appl. Sci.* **2019**, *9* (11), 2205. <https://doi.org/10.3390/app9112205>.
- [11] *Biofoams: Science and Applications of Bio-Based Cellular and Porous Materials*; Iannace, S., Park, C. B., Eds.; CRC Press: Boca Raton, 2016.
- [12] East, B.; Plencner, M.; Kralovic, M.; Rampichova, M.; Sovkova, V.; Vocetkova, K.; Otahal, M.; Tonar, Z.; Kolinko, Y.; Amler, E.; Hoch, J. A Polypropylene Mesh Modified with Poly- ϵ -Caprolactone Nanofibers in Hernia Repair: Large Animal Experiment. *Int. J. Nanomedicine* **2018**, *13*, 3129–3143. <https://doi.org/10.2147/IJN.S159480>.
- [13] Carrino, L.; Moroni, G.; Polini, W. Cold Plasma Treatment of Polypropylene Surface: A Study on Wettability and Adhesion. *J. Mater. Process. Technol.* **2002**, *121* (2), 373–382. [https://doi.org/10.1016/S0924-0136\(01\)01221-3](https://doi.org/10.1016/S0924-0136(01)01221-3).
- [14] Bhattacharya, A.; Misra, B. N. Grafting: A Versatile Means to Modify Polymers: Techniques, Factors and Applications. *Prog. Polym. Sci.* **2004**, *29* (8), 767–814. <https://doi.org/10.1016/j.progpolymsci.2004.05.002>.
- [15] Dufay, M.; Jimenez, M.; Degoutin, S. Effect of Cold Plasma Treatment on Electrospun Nanofibers Properties a Review. *ACS Appl. Bio Mater.* **2020**. In press.
- [16] Manakhov, A.; Kedroňová, E.; Medalová, J.; Černochová, P.; Obrusník, A.; Michlíček, M.; Shtansky, D. V.; Zajíčková, L. Carboxyl-Anhydride and Amine Plasma Coating of PCL Nanofibers to Improve Their Bioactivity. *Mater. Des.* **2017**, *132*, 257–265. <https://doi.org/10.1016/j.matdes.2017.06.057>.
- [17] Techaikool, P.; Daranarong, D.; Kongsuk, J.; Boonyawan, D.; Haron, N.; Harley, W. S.; Thomson, K. A.; Foster, L. J. R.; Punyodom, W. Effects of Plasma Treatment on Biocompatibility of Poly[(L-Lactide)-Co-(ϵ -Caprolactone)] and Poly[(L-Lactide)-Co-Glycolide] Electrospun Nanofibrous

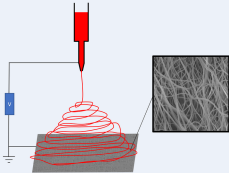
- Membranes - Techaikool - 2017 - Polymer International - Wiley Online Library. *Polym. Int.* **2017**, *66*, 1640–1650.
- [18] Heidari-Keshel, S.; Ahmadian, M.; Biazar, E.; Gazmeh, A.; Rabiei, M.; Adibi, M.; Soufi M, A.; Shabani, M. Surface Modification of Poly Hydroxybutyrate (PHB) Nanofibrous Mat by Collagen Protein and Its Cellular Study. *Mater. Technol.* **2016**, *31* (13), 799–805. <https://doi.org/10.1080/10667857.2016.1258517>.
- [19] Caton, J. G.; Zander, H. A. The Attachment Between Tooth and Gingival Tissues After Periodic Root Planing and Soft Tissue Curettage. *J. Periodontol.* **1979**, *50* (9), 462–466. <https://doi.org/10.1902/jop.1979.50.9.462>.
- [20] Permyakova, E. S.; Polčák, J.; Slukin, P. V.; Ignatov, S. G.; Gloushankova, N. A.; Zajíčková, L.; Shtansky, D. V.; Manakhov, A. Antibacterial Biocompatible PCL Nanofibers Modified by COOH-Anhydride Plasma Polymers and Gentamicin Immobilization. *Mater. Des.* **2018**, *153*, 60–70. <https://doi.org/10.1016/j.matdes.2018.05.002>.
- [21] Lü, L.; Deegan, A.; Musa, F.; Xu, T.; Yang, Y. The Effects of Biomimetically Conjugated VEGF on Osteogenesis and Angiogenesis of MSCs (Human and Rat) and HUVECs Co-Culture Models. *Colloids Surf. B Biointerfaces* **2018**, *167*, 550–559. <https://doi.org/10.1016/j.colsurfb.2018.04.060>.
- [22] Mahmoodinia Maymand, M.; Soleimanpour-Lichaei, H. R.; Ardeshirylajimi, A.; Soleimani, M.; Mirzaei, S.; Hajarizadeh, A.; Kabir Salmani, M. Hepatogenic Differentiation of Human Induced Pluripotent Stem Cells on Collagen-Coated Polyethersulfone Nanofibers. *ASAIO J. Am. Soc. Artif. Intern. Organs* **2017**, [1] Postoperative adhesion development after operative laparoscopy: evaluation at early second-look procedures**Presented in part at the 46th Annual Meeting of The American Fertility Society, Washington D.C., October 15 to 18, 1990., *Fertil. Steril.* *55* (1991) 700–704. [https://doi.org/10.1016/S0015-0282\(16\)54233-2](https://doi.org/10.1016/S0015-0282(16)54233-2).
- [2] A. Rocca, G. Aprea, G. Surfaro, M. Amato, A. Giuliani, M. Paccone, A. Salzano, A. Russo, D. Tafuri, B. Amato, Prevention and treatment of peritoneal adhesions in patients affected by vascular diseases following surgery: a review of the literature, *Open Med. Wars. Pol.* *11* (2016) 106–114. <https://doi.org/10.1515/med-2016-0021>.
- [3] Y.C. Cheong, S.M. Laird, T.C. Li, J.B. Shelton, W.L. Ledger, I.D. Cooke, Peritoneal healing and adhesion formation/reformation, *Hum. Reprod. Update.* *7* (2001) 556–566. <https://doi.org/10.1093/humupd/7.6.556>.
- [4] D.B. Johns, G.M. Keyport, F. Hoehler, G.S. diZerega, Intergel Adhesion Prevention Study Group, Reduction of postsurgical adhesions with Intergel adhesion prevention solution: a multicenter study of safety and efficacy after conservative gynecologic surgery, *Fertil. Steril.* *76* (2001) 595–604. [https://doi.org/10.1016/s0015-0282\(01\)01954-9](https://doi.org/10.1016/s0015-0282(01)01954-9).
- [5] J.M. Becker, M.T. Dayton, V.W. Fazio, D.E. Beck, S.J. Stryker, S.D. Wexner, B.G. Wolff, P.L. Roberts, L.E. Smith, S.A. Sweeney, M. Moore, Prevention of postoperative abdominal adhesions by a sodium hyaluronate-based bioresorbable membrane: a prospective, randomized, double-blind multicenter study, *J. Am. Coll. Surg.* *183* (1996) 297–306.
- [6] L. Mettler, A. Audebert, E. Lehmann-Willenbrock, K. Schive-Peterhansl, V.R. Jacobs, A randomized, prospective, controlled, multicenter clinical trial of a sprayable, site-specific adhesion barrier system in patients undergoing myomectomy, *Fertil. Steril.* *82* (2004) 398–404. <https://doi.org/10.1016/j.fertnstert.2003.12.046>.
- [7] R.M. Kamel, Prevention of postoperative peritoneal adhesions, *Eur. J. Obstet. Gynecol. Reprod. Biol.* *150* (2010) 111–118. <https://doi.org/10.1016/j.ejogrb.2010.02.003>.
- [8] A. Soundararajan, J. Muralidhar R, R. Dhandapani, J. Radhakrishnan, A. Manigandan, S. Kalyanasundaram, S. Sethuraman, A. Subramanian, Surface topography of polylactic acid nanofibrous mats: influence on blood compatibility, *J. Mater. Sci. Mater. Med.* *29* (2018) 145. <https://doi.org/10.1007/s10856-018-6153-2>.
- [9] P. Gentile, V. Chiono, I. Carmagnola, P.V. Hatton, An overview of poly(lactic-co-glycolic) acid (PLGA)-based biomaterials for bone tissue engineering, *Int. J. Mol. Sci.* *15* (2014) 3640–3659. <https://doi.org/10.3390/ijms15033640>.

- [10] M.J. Mochane, T.S. Motsoeneng, E.R. Sadiku, T.C. Mokhena, J.S. Sefadi, Morphology and Properties of Electrospun PCL and Its Composites for Medical Applications: A Mini Review, *Appl. Sci.* 9 (2019) 2205. <https://doi.org/10.3390/app9112205>.
- [11] S. Iannace, C.B. Park, eds., *Biofoams: science and applications of bio-based cellular and porous materials*, CRC Press, Boca Raton, 2016.
- [12] B. East, M. Plencner, M. Kralovic, M. Rampichova, V. Sovkova, K. Vocetkova, M. Otahal, Z. Tonar, Y. Kolinko, E. Amler, J. Hoch, A polypropylene mesh modified with poly- ϵ -caprolactone nanofibers in hernia repair: large animal experiment, *Int. J. Nanomedicine.* 13 (2018) 3129–3143. <https://doi.org/10.2147/IJN.S159480>.
- [13] L. Carrino, G. Moroni, W. Polini, Cold plasma treatment of polypropylene surface: a study on wettability and adhesion, *J. Mater. Process. Technol.* 121 (2002) 373–382. [https://doi.org/10.1016/S0924-0136\(01\)01221-3](https://doi.org/10.1016/S0924-0136(01)01221-3).
- [14] A. Bhattacharya, B.N. Misra, Grafting: a versatile means to modify polymers: Techniques, factors and applications, *Prog. Polym. Sci.* 29 (2004) 767–814. <https://doi.org/10.1016/j.progpolymsci.2004.05.002>.
- [15] M. Dufay, M. Jimenez, S. Degoutin, Effect of cold plasma treatment on electrospun nanofibers properties a review, *ACS Appl. Bio Mater.* (2020).
- [16] A. Manakhov, E. Kedroňová, J. Medalová, P. Černochová, A. Obrusník, M. Michlíček, D.V. Shtansky, L. Zajíčková, Carboxyl-anhydride and amine plasma coating of PCL nanofibers to improve their bioactivity, *Mater. Des.* 132 (2017) 257–265. <https://doi.org/10.1016/j.matdes.2017.06.057>.
- [17] P. Techaikool, D. Daranarong, J. Kongsuk, D. Boonyawan, N. Haron, W.S. Harley, K.A. Thomson, L.J.R. Foster, W. Punyodom, Effects of plasma treatment on biocompatibility of poly[(L-lactide)-co-(ϵ -caprolactone)] and poly[(L-lactide)-co-glycolide] electrospun nanofibrous membranes - Techaikool - 2017 - Polymer International - Wiley Online Library, *Polym. Int.* 66 (2017) 1640–1650.
- [18] S. Heidari-Keshel, M. Ahmadian, E. Biazar, A. Gazmeh, M. Rabiei, M. Adibi, A. Soufi M, M. Shabani, Surface modification of Poly Hydroxybutyrate (PHB) nanofibrous mat by collagen protein and its cellular study, *Mater. Technol.* 31 (2016) 799–805. <https://doi.org/10.1080/10667857.2016.1258517>.
- [19] J.G. Caton, H.A. Zander, The Attachment Between Tooth and Gingival Tissues After Periodic Root Planing and Soft Tissue Curettage, *J. Periodontol.* 50 (1979) 462–466. <https://doi.org/10.1902/jop.1979.50.9.462>.
- [20] E.S. Permyakova, J. Polčák, P.V. Slukin, S.G. Ignatov, N.A. Gloushankova, L. Zajíčková, D.V. Shtansky, A. Manakhov, Antibacterial biocompatible PCL nanofibers modified by COOH-anhydride plasma polymers and gentamicin immobilization, *Mater. Des.* 153 (2018) 60–70. <https://doi.org/10.1016/j.matdes.2018.05.002>.
- [21] L. Lü, A. Deegan, F. Musa, T. Xu, Y. Yang, The effects of biomimetically conjugated VEGF on osteogenesis and angiogenesis of MSCs (human and rat) and HUVECs co-culture models, *Colloids Surf. B Biointerfaces.* 167 (2018) 550–559. <https://doi.org/10.1016/j.colsurfb.2018.04.060>.
- [22] M. Mahmoodinia Maymand, H.R. Soleimanpour-Lichaei, A. Ardeshiryajimi, M. Soleimani, S. Mirzaei, A. Hajarizadeh, M. Kabir Salmani, Hepatogenic Differentiation of Human Induced Pluripotent Stem cells on Collagen-Coated Polyethersulfone Nanofibers, *ASAIO J. Am. Soc. Artif. Intern. Organs* 1992. 63 (2017) 316–323. <https://doi.org/10.1097/MAT.0000000000000469>.
- [23] E. Kedroňová, L. Zajíčková, D. Hegemann, M. Klíma, M. Michlíček, A. Manakhov, Plasma Enhanced CVD of Organosilicon Thin Films on Electrospun Polymer Nanofibers, *Plasma Process. Polym.* 12 (2015) 1231–1243. <https://doi.org/10.1002/ppap.201400235>.
- [24] M. Shao, L. Chen, Q. Yang, Preparation and surface modification of electrospun aligned poly(butylene carbonate) nanofibers, *J. Appl. Polym. Sci.* 130 (2013) 411–418. <https://doi.org/10.1002/app.39103>.

- [25] N. Blanchemain, M.R. Aguilar, F. Chai, M. Jimenez, E. Jean-Baptiste, A. El-Achari, B. Martel, H.F. Hildebrand, J.S. Roman, Selective biological response of human pulmonary microvascular endothelial cells and human pulmonary artery smooth muscle cells on cold-plasma-modified polyester vascular prostheses, *Biomed. Mater. Bristol Engl.* 6 (2011) 065003. <https://doi.org/10.1088/1748-6041/6/6/065003>.
- [26] G. Vermet, S. Degoutin, F. Chai, M. Maton, C. Flores, C. Neut, P.E. Danjou, B. Martel, N. Blanchemain, Cyclodextrin modified PLLA parietal reinforcement implant with prolonged antibacterial activity, *Acta Biomater.* 53 (2017) 222–232. <https://doi.org/10.1016/j.actbio.2017.02.017>.
- [27] BIOPHEN, BIOPHEN HEPARIN ANTI-Xa (2 stages) REF: 221010, (2015). <https://www.coachrom.com/fileadmin/docs/hbm/en/221010.pdf> (accessed April 27, 2020).
- [28] M. Putti, M. Simonet, R. Solberg, G.W.M. Peters, Electrospinning poly(ϵ -caprolactone) under controlled environmental conditions: Influence on fiber morphology and orientation, *Polymer.* 63 (2015) 189–195. <https://doi.org/10.1016/j.polymer.2015.03.006>.
- [29] L. Liverani, J. Lacina, J.A. Roether, E. Boccardi, M.S. Killian, P. Schmuki, D.W. Schubert, A.R. Boccaccini, Incorporation of bioactive glass nanoparticles in electrospun PCL/chitosan fibers by using benign solvents, *Bioact. Mater.* (2017). <https://doi.org/10.1016/j.bioactmat.2017.05.003>.
- [30] S. Degoutin, M. Jimenez, M. Casetta, S. Bellayer, F. Chai, N. Blanchemain, C. Neut, I. Kacem, M. Traisnel, B. Martel, Anticoagulant and antimicrobial finishing of non-woven polypropylene textiles, *Biomed. Mater. Bristol Engl.* 7 (2012) 035001. <https://doi.org/10.1088/1748-6041/7/3/035001>.
- [31] N. Blanchemain, M.R. Aguilar, F. Chai, M. Jimenez, E. Jean-Baptiste, A. El-Achari, B. Martel, H.F. Hildebrand, J.S. Roman, Selective biological response of human pulmonary microvascular endothelial cells and human pulmonary artery smooth muscle cells on cold-plasma-modified polyester vascular prostheses, *Biomed. Mater. Bristol Engl.* 6 (2011) 065003. <https://doi.org/10.1088/1748-6041/6/6/065003>.
- 63 (3), 316–323. <https://doi.org/10.1097/MAT.0000000000000469>.
- [23] Kedroňová, E.; Zajíčková, L.; Hegemann, D.; Klíma, M.; Michlíček, M.; Manakhov, A. Plasma Enhanced CVD of Organosilicon Thin Films on Electrospun Polymer Nanofibers. *Plasma Process. Polym.* 2015, 12 (11), 1231–1243. <https://doi.org/10.1002/ppap.201400235>.
- [24] Shao, M.; Chen, L.; Yang, Q. Preparation and Surface Modification of Electrospun Aligned Poly(Butylene Carbonate) Nanofibers. *J. Appl. Polym. Sci.* 2013, 130 (1), 411–418. <https://doi.org/10.1002/app.39103>.
- [25] Blanchemain, N.; Aguilar, M. R.; Chai, F.; Jimenez, M.; Jean-Baptiste, E.; El-Achari, A.; Martel, B.; Hildebrand, H. F.; Roman, J. S. Selective Biological Response of Human Pulmonary Microvascular Endothelial Cells and Human Pulmonary Artery Smooth Muscle Cells on Cold-Plasma-Modified Polyester Vascular Prostheses. *Biomed. Mater. Bristol Engl.* 2011, 6 (6), 065003. <https://doi.org/10.1088/1748-6041/6/6/065003>.
- [26] Vermet, G.; Degoutin, S.; Chai, F.; Maton, M.; Flores, C.; Neut, C.; Danjou, P. E.; Martel, B.; Blanchemain, N. Cyclodextrin Modified PLLA Parietal Reinforcement Implant with Prolonged Antibacterial Activity. *Acta Biomater.* 2017, 53, 222–232. <https://doi.org/10.1016/j.actbio.2017.02.017>.
- [27] BIOPHEN. BIOPHEN HEPARIN ANTI-Xa (2 Stages) REF: 221010. 2015.
- [28] Putti, M.; Simonet, M.; Solberg, R.; Peters, G. W. M. Electrospinning Poly(ϵ -Caprolactone) under Controlled Environmental Conditions: Influence on Fiber Morphology and Orientation. *Polymer* 2015, 63 (Supplement C), 189–195. <https://doi.org/10.1016/j.polymer.2015.03.006>.
- [29] Liverani, L.; Lacina, J.; Roether, J. A.; Boccardi, E.; Killian, M. S.; Schmuki, P.; Schubert, D. W.; Boccaccini, A. R. Incorporation of Bioactive Glass Nanoparticles in Electrospun PCL/Chitosan Fibers by Using Benign Solvents. *Bioact. Mater.* 2017. <https://doi.org/10.1016/j.bioactmat.2017.05.003>.
- [30] Degoutin, S.; Jimenez, M.; Casetta, M.; Bellayer, S.; Chai, F.; Blanchemain, N.; Neut, C.; Kacem, I.; Traisnel, M.; Martel, B. Anticoagulant and Antimicrobial Finishing of Non-Woven Polypropylene

Textiles. *Biomed. Mater. Bristol Engl.* **2012**, 7 (3), 035001. <https://doi.org/10.1088/1748-6041/7/3/035001>.

Electrospinning



Cold plasma

